Accepted Manuscript

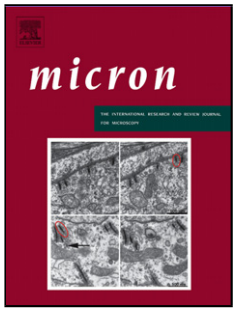

Title: Effect of extract from ginseng rust rot on the inhibition of human hepatocellular carcinoma cells *in vitro*

Authors: Jing Hu, Jie Jiao, Ying Wang, Mingyan Gao, Zhengcheng Lu, Fan Yang, Cuihua Hu, Zhengxun Song, Yujuan Chen, Zuobin Wang

PII: S0968-4328(19)30133-7
DOI: https://doi.org/10.1016/j.micron.2019.102710
Article Number: 102710

Reference: JMIC 102710

To appear in: *Micron*

Received date: 18 April 2019
Revised date: 28 June 2019
Accepted date: 1 July 2019

Please cite this article as: Hu J, Jiao J, Wang Y, Gao M, Lu Z, Yang F, Hu C, Song Z, Chen Y, Wang Z, Effect of extract from ginseng rust rot on the inhibition of human hepatocellular carcinoma cells *in vitro*, *Micron* (2019), https://doi.org/10.1016/j.micron.2019.102710

Effect of extract from ginseng rust rot on the inhibition of human hepatocellular carcinoma cells *in vitro*

Jing Hu[a,b], Jie Jiao[a,b,c], Ying Wang[a,b], Mingyan Gao[a,b], Zhengcheng Lu[d], Fan Yang[a,b], Cuihua Hu[a,b], Zhengxun Song[a,b], Yujuan Chen[a,b,c*], Zuobin Wang[a,b,d*]

[a] *Ministry of Education Key Laboratory for Cross-Scale Micro and Nano Manufacturing, Changchun University of Science and Technology, Changchun 130022, China*

[b] *International Research Centre for Nano Handling and Manufacturing of China, Changchun University of Science and Technology, Changchun 130022, China*

[c] *School of Life Sciences, Changchun University of Science and Technology, Changchun 130022, China*

[d] *JR3CN & IRAC, University of Bedfordshire, Luton LU1 3JU, UK*

Corresponding author

To whom correspondence should be addressed.

E-mail: wangz@cust.edu.cn (Z.W.); chenyujuan@cust.edu.cn (Y.C.).

Tel./Fax: +86-0431-85360138.

Highlights

- Toxic were examined in human liver cancer cells and human normal liver cells.
- Cells morphologies were analyzed by employing multiple methods.
- Ginseng rust rot epidermis shows enhanced anti-cancer activity and little toxicity.
- Anti-cancer action was ascribed to the collapse of the cellular membrane in cells.

Abstract

Hepatocellular carcinoma (HCC) is one of major leading causes of cancer death worldwide. As a traditional medicine, the anti-cancer function of ginseng is being growingly recognized and investigated. However, the effect of ginseng rust rot on human HCC is unknown yet. In this study, the HCC cells were treated with different parts of mountain cultivated ginseng rust rot and compared with human normal liver cells. The morphology, survival rate and β-actin expression of the cells were changed by introducing the ginseng epidermis during the incubation process. Notably, the results reveal that the ginseng epidermis can induce apoptosis by altering the morphologies of cells, indicating the practical implication for the HCC treatment and drug development.

Abbreviations: HCC, hepatocellular carcinoma; GR, ginseng roots; GE, ginseng epidermis; GWE, ginseng roots without epidermis

Keywords: Ginseng-extracted compounds; anti-tumor effect; hepatocelluar carcinoma

1. Introduction

Cancer, which is uncontrolled, invasive and sometimes metastasizing, gives us the creeps (Tai et al., 2010). Over recent years, cancer is one of the major global diseases that has depicted a drastic increase in morbidity and mortality rates (Pang et al., 2018; Gao et al., 2018). There are many factors causing the problem of cancer development, such as inheritance, obesity, smoking, infection, physical inactivity and even negative emotion (Torre et al., 2012; Ferlay et al., 2015). Among various cancers, hepatocellular carcinoma (HCC) has been regarded as the most frequently malignant tumor worldwide due to its aggressive malignance and high prevalence (Yoon et al., 2012). Currently, chemotherapy or radiotherapy is the mainstay for tumor therapy, which not only directly kills tumor cells but also damages normal cells (Fox et al., 2016). As a result, patients have many symptoms including vomiting, nausea, pain, fatigue, anemia, anorexia, hair loss and poor quality of life (Wong et al., 2015; Kashinath et al., 2013). Therefore, finding potent complementary and alternative medicines with few adverse effects has become growingly urgent for cancer treatments.

It has been reported that natural compounds from plants are becoming popular alternative medicines with remarkable bioactivities and minimal toxicity (Ahuja et al., 2018; Hyemin et al., 2012). Moreover, tremendous efforts have been made to study the efficacy of ginseng about the apoptosis of cancer cells (Qi et al., 2011; Lee et al., 2018;

Kim et al., 2018). Ginseng occupies a prominent position as a medicinal herb and has been widely used for thousands of years in North America and Asian countries (Wang et al., 2015). It has attracted increasing attention as a natural product with a variety of pharmacological activities including anti-tumor, anti-shock, anti-fatigue, anti-oxidant and anti-inflammatory (Christensen 2009). According to the literature, ginseng cultivated and grown in naturally mountainous forests is named "mountain cultivated ginseng" (Kwon et al., 2011). However, in naturally mountainous environments, ginseng plants are vulnerable to be attacked by bacteria, fungi and nematodes during the cultivation, in which root rot is one of the most common diseases (Kim et al., 2017; Farh et al., 2018). Meanwhile, to the best of our knowledge, the anti-tumor activity of mountain cultivated ginseng rust rot has rarely been reported. Besides, it has been proved that the subtle mechanical or morphologic changes of the cells are crucial for the description of cell behaviors (Virjula et al., 2017; Kim et al.,2014).

In this work, the different constituents of mountain cultivated ginseng rust rot were extracted and their cytotoxicity on human liver cancer cells and human normal liver cells was examined. The morphologies of the cells before and after the treatment with ginseng epidermis were also analyzed by employing multiple methods. In addition, the possible anti-cancer mechanism was explored.

2. Materials and methods

2.1. Chemicals

RPMI 1640 medium and fetal bovine serum (FBS) were obtained from Hyclone

Laboratories Inc., (Waltham, USA). 3-(4, 5-dimethylthiazol-2-yl)-2, 5-diphenyltetrazolium bromide (MTT) and dimethyl sulfoxide (DMSO) were purchased from Solarbio Science & Technology Ltd., (Beijing, China). Trypsin was from Sigma-Aldrich Inc., (Milwaukee, USA). Anti-ACTA2 antibody and HRP-conjugated Rabbit anti-mouse lgG were purchased from BBI-Life Sciences Co., (Beijing, China). Other reagents were of at least analytical grade and used as received without further purification.

2.2. Plant material and extract preparation

The mountain cultivated ginseng rust rot was collected from Changbai Mountain in the northeast of China. Briefly, the ginseng roots, the epidermis and the roots without epidermis were cut into small pieces and extracted with 95% ethanol at 110 ^{o}C for 6 h by soxhlet extractor, respectively. After cooling to room temperature, the resulting products were collected by vacuum freeze-drying and named as GR, GE and GWE, respectively. Furthermore, the micro and nano structures of GR, GE and GWE were examined by scanning electron microscope (SEM, Quanta 250).

2.3. Cell culture

Human normal liver cells (HL-7702) were grown with RPMI 1640 medium containing 15% FBS, and human liver cancer cells (SMMC-7721 and HepG2) were cultured in RPMI 1640 medium supplemented with 10% FBS. In this study, all cells were incubated with 5% CO_2 at 37 ^{o}C.

2.4. Cell viability assays

The logarithmic growth phase of HL-7702, SMMC-7721 and HepG2 cells were seeded into 96-well plates with the density of 6×10^3 cells per well. After adhering to the surface, cells were treated with GR, GE and GWE at various concentrations (0, 30.75, 61.5, 125, 250 and 500 μg mL^{-1}) for 48 h. Thereafter, 20 μL of 1 mg mL^{-1} MTT solution in phosphate (PBS) was individually added to each well. After incubated for other 4 h at 37 ºC, the solution was carefully removed and replaced by 150 μL DMSO. The OD value was determined at the wavelength of 490 nm. The cell viability assays were repeated in triplicates and the cell viability can be calculated using the following equation: Cell viability (%) $=OD_{sample} / OD_{control}\times100\%$, where OD_{sample} represents the average OD value of the cells treated with GR, GE and GWE, and $OD_{control}$ is the average OD value of the cells treated without GR, GE and GWE.

2.5. Scanning electron microscopy

HL-7702, SMMC-7721 and HepG2 cells were prepared according to the early literature with some modifications (Huang et al., 2011). In a typical procedure, sterilized coverslips were first placed into 12-well plates. Approximately 3×10^4 cells were plated onto each well in 1 mL RPMI 1640 medium and incubated under the same conditions as described above. Different concentrations of GE (0, 50, 100 and 200 μg mL^{-1}) were added and the cells were incubated at 37 ºC for 24 h. The medium was then removed and subsequently 1 mL 4 % glutaraldehyde solution was added to each well staying overnight. All coverslips were washed several times with the PBS and

dehydrated in ethanol. The coverslips were then immersed in tertiary butyl alcohol overnight. The resulting coverslips were dried in a critical point dryer and coated with 1.5 nm gold for scanning electron microscopy (SEM) imaging.

2.6. Inverted microscopy

In the experiments, the method of cell culture was the same as mentioned in the section of scanning electron microscopy. Briefly, 3×10^4 cells per well were seeded into 12-well plates in 1 mL RPMI 1640 medium and incubated. Cells were exposed to GE solutions with the different concentrations 0, 50, 100 and 200 μg mL^{-1} for 24 h. The medium was then removed and washed by PBS buffer. The cell morphologies were observed by inverted microscope.

2.7. Atomic force microscopy

The process to prepare the HL-7702, SMMC-7721 and HepG2 samples for an atomic force microscope (AFM) was similar to that for the SEM samples without gold coating. Finally, the cells were detected by AFM (Agilent technologies, 5500) for imaging.

2.8. Western blotting

After the incubation of the HL-7702, SMMC-7721 and HepG2 cells in 6-well plates (1×10^6 per well), the cells were treated with GE (0, 100, 150, 200 and 250 μg mL^{-1}). After 24 h incubation, the harvested cells by 0.25 % trypsin were thawed and refrozen three times in the PBS buffer and then centrifuged (10000 rpm, 10 min),

collected and heated for 7 min at 100 ^{o}C. Typically, the same number of cell supernatants were loaded onto a 10% SDS-PAGE and electrotransferred to a polyvinylidene fluoride (PVDF) membrane. The membrane was then blocked with 5% bovine serum albumin (BSA) for 1 h and incubated overnight with Anti-ACTA2 antibody (1:5000) at 4 ^{o}C. After washed by PBST for three times, the membrane was incubated with HRP-conjugated Rabbit anti-mouse lgG (1:5000) for 1 h at room temperature. The bands were visualized using the DAB method. The number of cells was confirmed by a Nexcelom cellometer.

2.9. Statistical analysis

Experimental data were expressed as means ± the standard error of the mean (S.E.M.). All statistical analyses were analyzed by GraphPad Prism 5 (GraphPad Software Inc., USA). A p value < 0.05 was considered to be statistically significant.

3. Results

3.1. The ultrastructure of ginseng-extracted compounds

Here in, the typical SEM images of the obtained GR, GWE and GE powders after their dispersions in water are shown in Figs. 1A-1C. There are some white dots dispersed on the porous surfaces in Figs. 1A and 1B. Obviously, a plenty of randomly distributed roughly spherical particles are found in Fig. 1C compared with the GR and GWE.

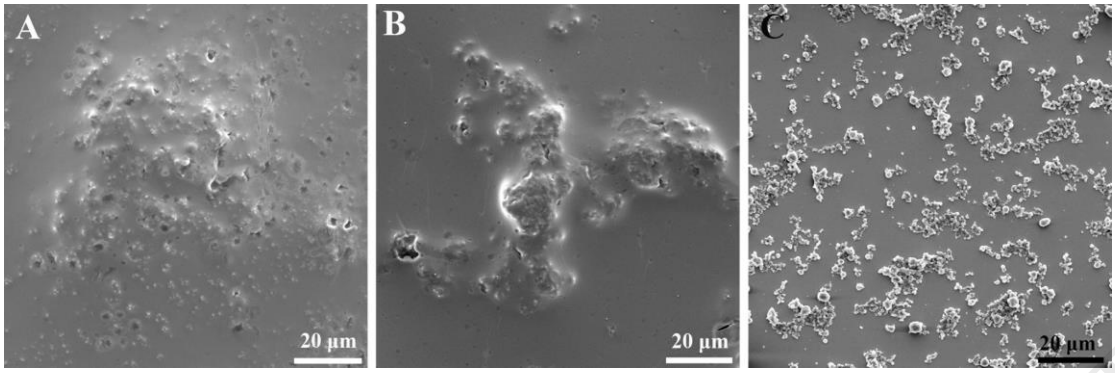

Fig. 1. Typical SEM images of GR (A), GWE (B) and GE (C).

3.2. Cell viability

MTT assay is a classical tool used for effectively evaluating cell survival rates. To explore the cytotoxic effects of as-extracted ginseng-derived compounds on the cells, SMMC-7721 and HepG2 cells were incubated with the increased concentrations of GR, GWE and GE, and their viabilities were then measured by MTT assay. In addition, the effects of different samples on HL-7702 cells were also performed for comparison. Figs. 2A-2C show the cell viabilities of SMMC-7721, HepG2 and HL-7702 cells before and

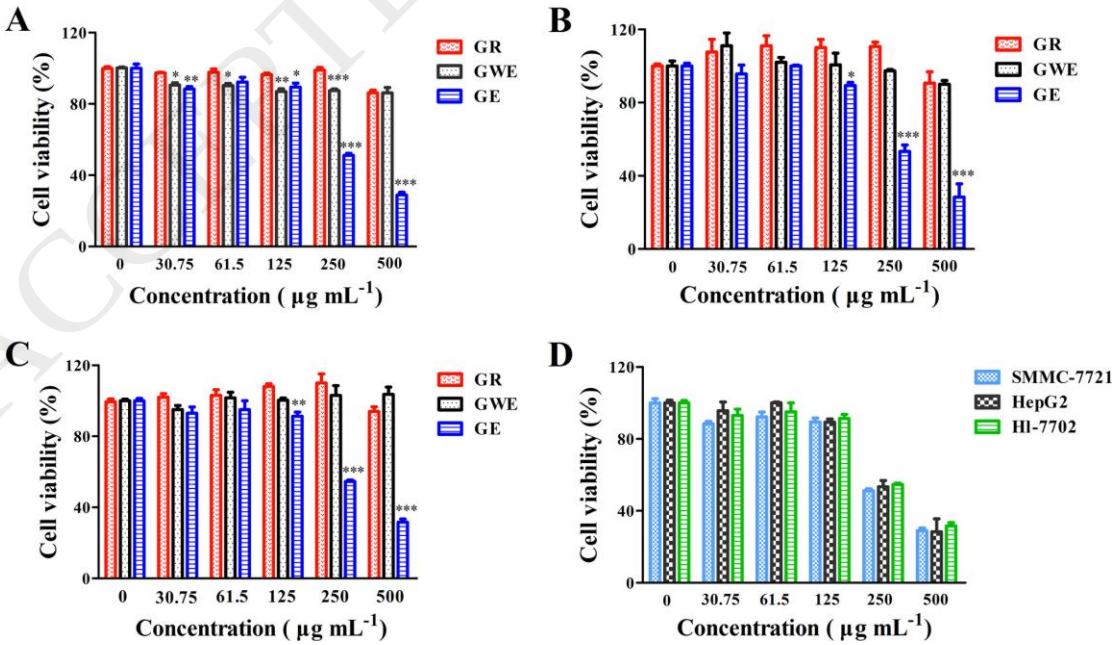

Fig. 2. The cell viability of SMMC-7721 (A), HepG2 (B) and HL-7702 (C) cells with different concentrations of GR, GWE and GE. The cell viability of SMMC-7721, HepG2 and HL-7702 cells with different concentrations of GE (D). The data are displayed as the mean ± S.E.M. of three independent experiments ($^{*}P<0.05$, $^{**}P<0.01$, $^{***}P<0.001$ when compared with different concentrate of GR).

after the treatments with GR and GE, respectively. Obviously, there were no distinct alterations on the three types of cells at the concentration range from 0 to 500 μg mL^{-1}, implying that GR and GWE had no obvious toxicity to human normal liver cells or liver cancer cells at the concentrations. However, it can be seen that the cell viability shows a slight change at first, and then significantly decreased after the treatment with GE at 125 μg mL^{-1}. Besides, the effect of GE on SMMC-7721, HepG2 and HL-7702 cells was further compared. As shown in Fig. 2D, the survival rate of HL-7702 (91.3%) cells was just marginally greater than those of HepG2 (89.3%) and SMMC-7721 (89.5%) cells when the GE concentration was 125 μg mL^{-1}. With the increase of GE concentration (250 μg mL^{-1}), the survival rate of HL-7702 (54.7%) cells was gradually higher than those of HepG2 (53.3%) and SMMC-7721 (51.1%) cells. When the GE concentration was increased to 500 μg mL^{-1}, the maximum survival rate of HL-7702 (31.7%) cells was about 1.12 and 1.09 times of the corresponding value for HepG2 (28.3%) and SMMC-7721 (29.0%) cells, respectively.

3.3. Cell morphology

The changes in cells on the nanoscale can be observed directly by morphological

analysis. Figs. 3, 4 and 5 depict the images of HL-7702, SMMC-7721 and HepG2 cells with or without the GE treatment observed by inverted microscope, SEM and AFM, respectively. Because the samples were prepared according to the different microscope methods used, each method may lead to distinctive artifacts (Yang et al., 2013). As shown in Fig. 3, the control cells were alive without GE. Whereas, the cell morphology changed visibly to become more unapparent when the GE concentration was increased from 50 μg mL^{-1} to 200 μg mL^{-1} and a gradual decrease in the number of cells was also observed. Furthermore, with the increase of GE, a lot of impurities including numerous densely distributed small particles as well as some obviously large particles appeared in the view. The presence of the impurities might be resulted from the production of cell metabolites, cellular debris or GE residues.

To obtain more detailed image information of the cells, SEM technology was applied. Remarkably, the untreated cells presented plenty of microvilli and the patterns

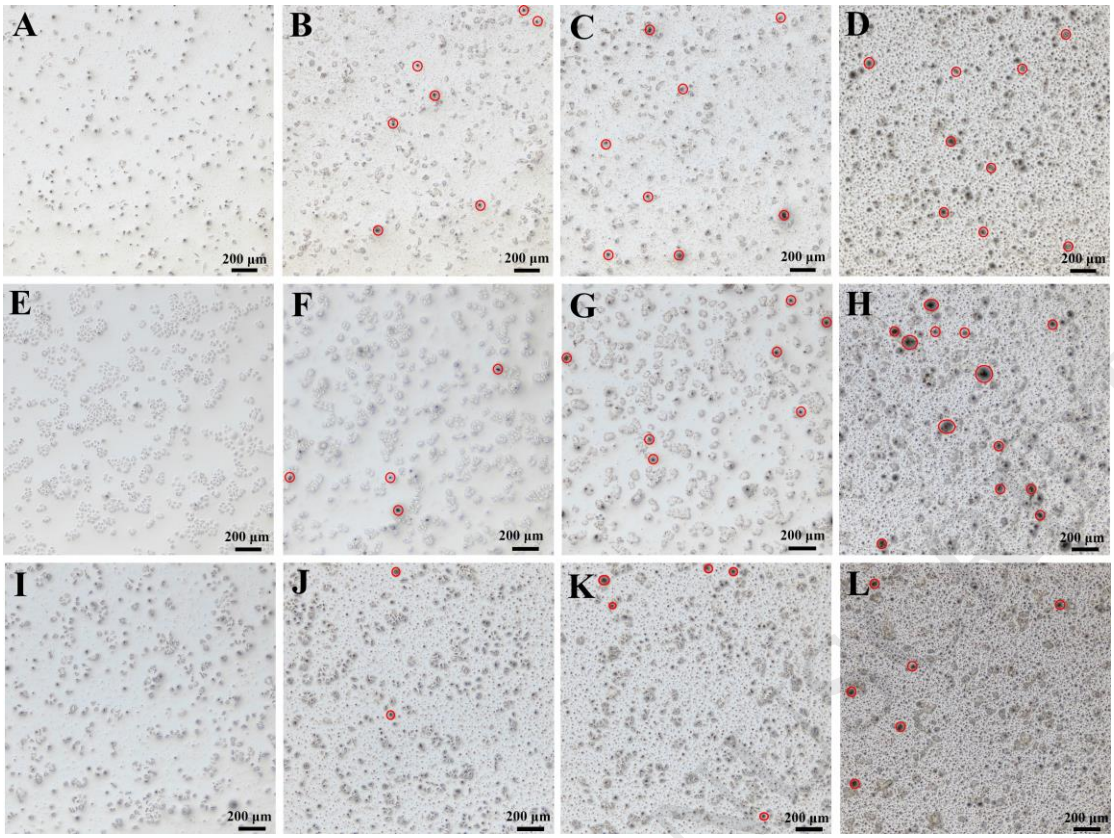

Fig. 3. Inverted microscope images of the HL-7702 (A-D), SMMC-7721 (E-H) and HepG2 (I-L) cells incubated with GE at 0 (A, E and I), 50 (B, F and J), 100 (C, G and K) and 200 μg mL^{-1} (D, H and L) for 24 h. The circles show the large particles of impurities.

were more regular (Figs. 4A, 4E and 4I). Along with the GE increasement, HL-7702, SMMC-7721 and HepG2 cells suggested collapsed cell membrane as well as aggravated cavity formation. Loss of membrane integrity and microvilli were also observed after the GE incubation, which could block the exchange of biological information between the cells and inhibit cell proliferation. Interestingly, the elongated shape of cells can be found on the images of three cells (Figs. 4D, 4H and 4L) after the GE (200 μg mL^{-1}) treatment. With the GE treatment going on, more and more chips

were seen in the images. The findings implied that the cellular membranes were dissolved.

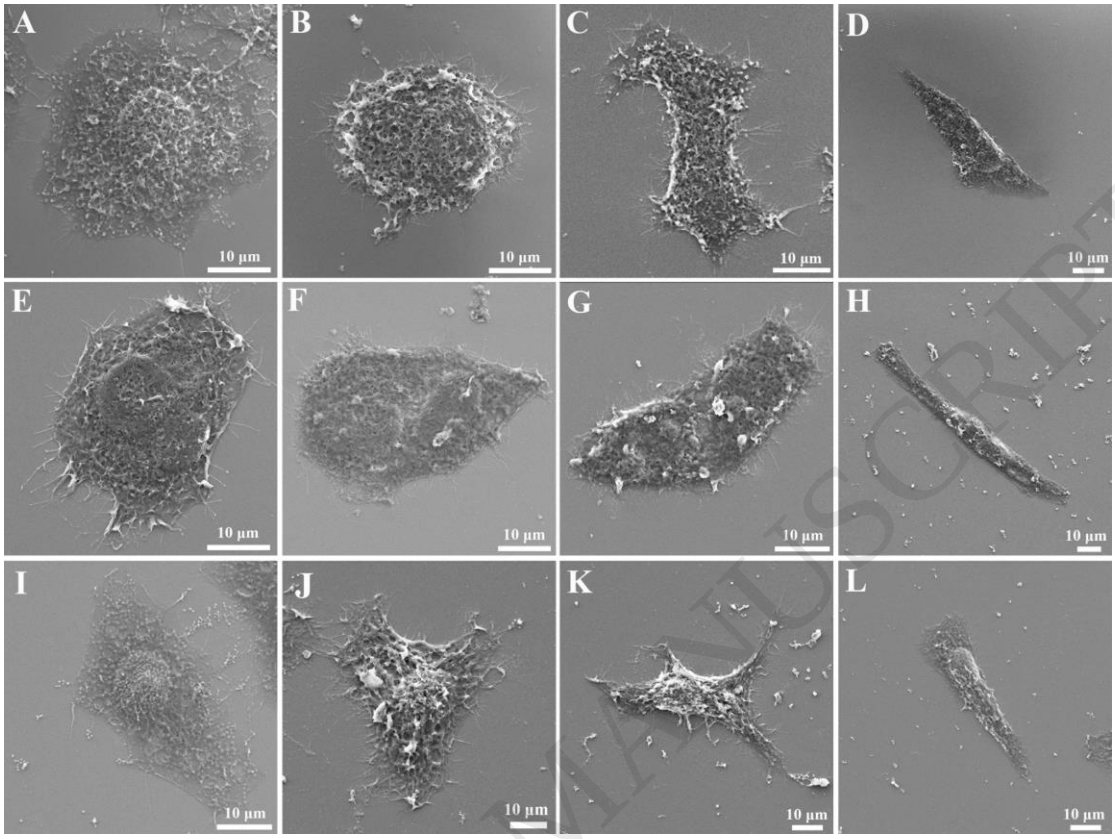

Fig. 4. SEM images of the HL-7702 (A-D), SMMC-7721 (E-H) and HepG2 (I-L) cells incubated with GE at 0 (A, E and I), 50 (B, F and J), 100 (C, G and K) and 200 μg mL^{-1} (D, H and L) for 24 h.

In recent years, AFM has been widely used in the study of cells due to its high sensitivity and reliability (Dong et al., 2007; Lazar et al., 2013; Li et al., 2014; Zhang et al., 2013; Alsteens et al., 2017; Krieg et al., 2018). A set of topography images of HL-7702, SMMC-7721 and HepG2 cells were investigated by AFM in the contact mode, as shown in Fig. 5. For the cells adhered to the coverslips, only a few metabolites and lots of intact cells were observed (Figs. 5A, 5E and 5I). After incubation with GE,

a large number of unique shape cells arose, in addition to a lot of wastes. Observation on the images showed that the morphological changes were embodied as increased in length and decreased in cell integrity, illustrating that the morphological changes were dose-dependent.

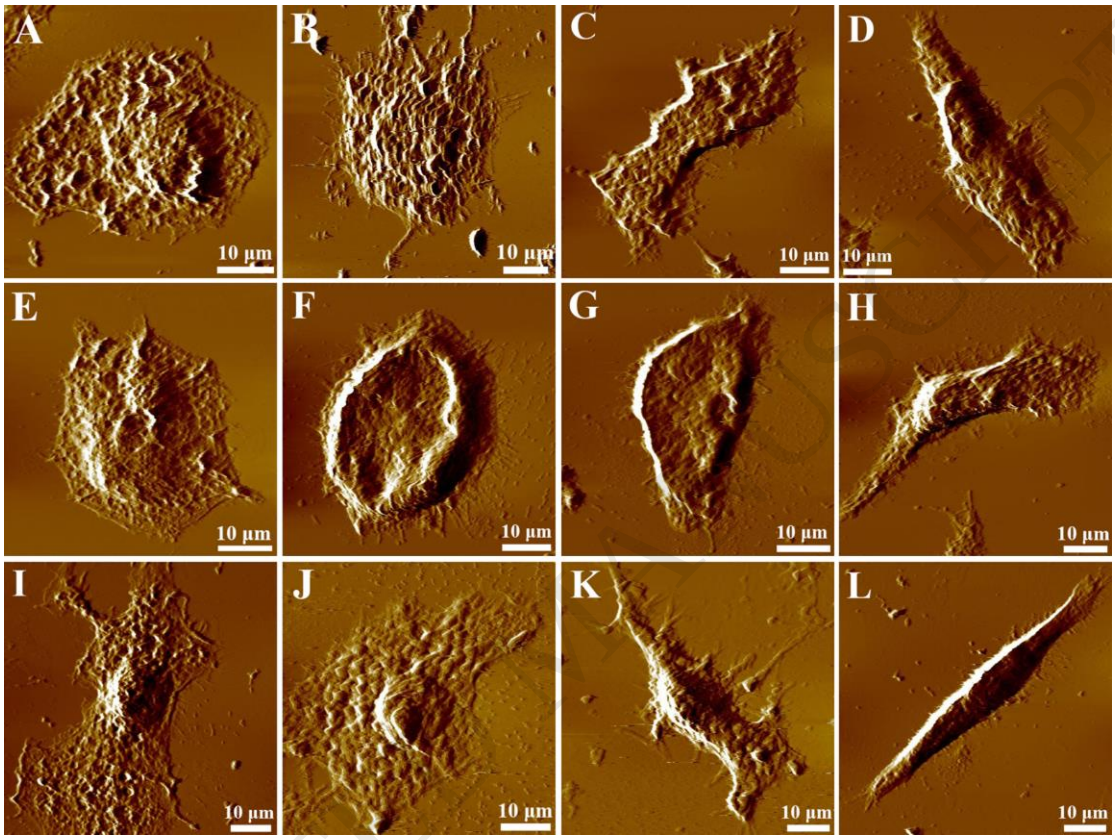

Fig. 5. AFM cantilever-deflection images of the HL-7702 (A-D), SMMC-7721 (E-H) and HepG2 (I-L) cells incubated with GE at 0 (A, E and I), 50 (B, F and J), 100 (C, G and K) and 200 μg mL^{-1} (D, H and L) for 24 h.

3.3. Analysis of western blotting

Western blot was one of the gold standard techniques for investigating the amount of individual proteins (Ma et al., 2014; Rajeshwary et al., 2014). In order to examine whether the GE influences the expression of *β*-actin, HepG2 and SMMC-7721 cells

were selected for the treatment with GE (0, 100, 150, 200 and 250 μg mL^{-1}) and incubated for 24 h. As displayed in Fig 6, GE-treated HepG2 and SMMC-7721 cells

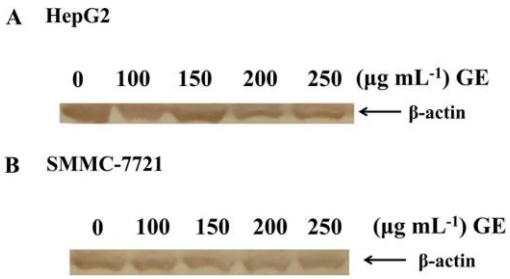

Fig. 6. Effects of GE on β-actin expression in HepG2 (A) and SMMC-7721 (B) cells. exhibited a reduction in *β*-actin expression with the raised concentration of GE.

4. Discussions

With the advances in pharmacology and phytology, the effect of ginseng is one of current research focuses in the field of cancer treatment and a wealth of valuable information have been reported (Nawab et al., 2015; Castroaceituno et al., 2016). However, ginseng is different in its effect and potency for anti-cancer functions due to various modes of action (Kang et al., 2011; Poudyal et al., 2013; Yu et al., 2017; Shi et al., 2018). Peralta et al. (2009) reported that ginseng exhibited its anti-cancer activity by the down-regulation of COX-2 expression in breast cancer cells. Wang et al. (2009) indicated that the mitochondrial pathway played a key role in the apoptosis of ginseng-mediated human colorectal cancer cells. Additionally, Park et al. (2016) reported that ginseng could suppress the proliferation of human prostate cancer cells.

In this study, GR, GE and GWE were extracted from mountain cultivated ginseng rust rot by heat processing. According to the SEM images, the random distribution

grains of GE and the irregular shapes of GR and GWE structures can be observed evidently. Besides, the results from the MTT indicated that the GE was less cytotoxic for HL-7702 cells than HepG2 and SMMC-7721 cells when the concentration was greater than 125 μg mL^{-1}. However, the GR and GWE had little inhibitory effect on HCC until 500 μg mL^{-1}. The different cytotoxic effects on the cells could be caused by different sizes of GR, GE and GWE from which the smaller GWE particles had shown stronger cytotoxicity. Thus, we speculated that GE could have a potential to induce the apoptosis of human liver cancer cells. This assumption was supported by the morphological changes in cells (Figs. 3, 4 and 5). The cell volume loss is a basic feature of programmed cell death (Bortner et al., 1998; Yang et al., 2010). The SEM as well as AFM results both clearly demonstrated that the cell deformation and membrane collapse with the increase of GE concentration. It was noted that when GE was absent, the morphologies of the three types of cells were normal and abundant. Therefore, the results revealed that the GE-induced damage of cell membrane was the main factor for the reduction of cell viability.

It is known that the cell apoptosis is closely related to proteins, such as membrane skeleton protein (Yang et al., 2010). Membrane skeleton protein is one of the two-dimensional proteins in most cell types and plays an important role in the cell shape, cytokinesis, secretion, protein organization and signal transduction pathway (Basu et al., 2015; Wang et al., 2010). In parallel, actin fulfills the intracellular transport, membrane dynamics and migration, adhesion and contraction as well as cell-cell contact regulation. All the cellular functions make actin a typical type of membrane

skeleton proteins (Melak et al., 2017). The results indicated that the expression of *β*-actin was downregulated after HepG2 and SMMC-7721 cells were treated with GE (Fig 6). It was reported that the dynamic regulation of actin cytoskeleton regulated the changes of cell morphology and the formation of adhesion structure (Wang et al., 2010). Hence, we hypothesised that the decrease of the *β*-actin modulated by GE could promote the apoptosis of HepG2 and SMMC-7721 cells. According to the results of morphology detection, cell viability and western blotting experiments, the GE could induce the cell apoptosis by changing cell morphology and suppressing communication between cells via destabilizing *β*-actin protein.

5. Conclusions

In summary, the epidermis of mountain cultivated ginseng rust rot exhibits enhanced anti-cancer activity and little toxicity to human normal liver cells than the ginseng roots and the ginseng roots without epidermis. The SEM results demonstrated that the ultrastructures of ginseng epidermis were composed mostly of randomly distributed ball-shaped particles, and the mechanism of anti-cancer actions of ginseng epidermis might be ascribed to the collapse of the cellular membrane in cells. Besides, western blotting analysis revealed that the expression of *β*-actin was decreased with the increase of ginseng epidermis concentration, further implying that the ginseng epidermis had a significant impact on the *β*-actin to induce the cell apoptosis. Thus, the as-extracted ginseng epidermis can be considered as a promising anti-tumor medicine with a potential application prospect in cancer treatments.

Conflict of interest

The authors declare that there is no conflict of interest.

Acknowledgement

This work was supported by National Key R&D Program of China (No.2017YFE0112100), EU H2020 Program (MNR4SCELL No.734174), Jilin Provincial Science and Technology Program (Nos. 20160623002TC, 20180414002GH, 20180414081GH, 20180520203JH and 20190702002GH), and "111" Project of China (D17017).

References

Ahuja, A., Ji, H.K., Kim, J.H., Yi, Y.S., Cho, J.Y., 2018. Functional role of ginseng-derived compounds in cancer. J Gins Res 42 (3), 248-254. https://doi.org/10.1016/j.jgr.2017.04.009.

Alsteens, D., Gaub, H.E., Newton, R., Pfreundschuh, M., Gerber, C., Müller, D.J., 2017. Atomic force microscopy-based characterization and design of biointerfaces. Nature Mater 2 (5), 17008. https://doi.org/10.1038/natrevmats.2017.8.

Basu, A., Harper, S., Pesciotta, E.N., Speicher, K.D., Chakrabarti, A., Speicher, D.W., 2015. Proteome analysis of the triton-insoluble erythrocyte membrane skeleton. J Proteomics 128, 298-305. https://doi.org/10.1016/j.jprot.2015.08.004.

Bortner, C.D., Cidlowski, J.A., 1998. A necessary role for cell shrinkage in apoptosis. Biochem Pharmacol. 56 (12), 1549-1559. https://doi.org/10.1016/S0006-2952(98)00225-1.

Castroaceituno, V., Ahn, S., Simu, S.Y., Singh, P., Mathiyalagan, R., Lee, H.A., Yang, D.C., 2016. Anticancer activity of silver nanoparticles from Panax ginseng fresh leaves in human cancer cells. Biomedicine & Pharmacotherapy, 84, 158-165. https://doi.org/10.1016/j.biopha.2016.09.016.

Christensen, L.P., 2009. Chapter 1 Ginsenosides : Chemistry, biosynthesis, analysis, and potential health effects. Adv Food Nutr Res 55 (55), 1-99. https://doi.org/10.1016/S1043-4526(08)00401-4.

Dong, M.D., Xu, S.l., Oliveira, C.L.P., Pedersen, J.S., Thiel, S., Besenbacher, F., Vorup-Jensen, T., 2007. Conformational changes in mannan-binding lectin bound to

ligand surfaces. J Immunol 178 (5), 3016-3022. https://doi.org/10.4049/jimmunol.178.5.3016.

Farh, E.A., Kim, Y.J., Yang D.C., 2018. Cylindrocarpon destructans/Ilyonectria radicicola-species complex: causative agent of ginseng root-rot disease and rusty symptoms. J Gins Res 42 (1), 9-15. https://doi.org/10.1016/j.jgr.2017.01.004.

Ferlay, J., Soerjomataram, I., Dikshit, R., Eser, S., Mathers, C., Rebelo, M., Parkin, D.M., Forman, D., Bray, F., 2015. Cancer incidence and mortality worldwide: sources, methods and major patterns in GLOBOCAN 2012. Int J Cancer 136 (5), E359-E386. https://doi.org/10.1002/ijc.29210.

Fox, J.L., Macfarlane, M., 2016. Targeting cell death signalling in cancer: minimising 'Collateral damage'. Brit J Cancer 115 (1), 5-11. https://doi.org/10.1038/bjc.2016.111.

Gao, Y.G., Liu, J.T., Ji, Q., Zhao, Y., Zang, P., He, Z.M., Zhu, H.Y., Zhang, L.X., 2018. Anti-tumor activity and related mechanism study of bacillus polymyxa transformed Panax ginseng C. A. Mey. Process Biochem 72, 198-208. https://doi.org/10.1016/j.procbio.2018.06.013.

Huang, Y.B., Wang, X.F., Wang, H.Y., Liu, Y., Chen, Y., 2011. Studies on mechanism of action of anticancer peptides by modulation of hydrophobicity within a defined structural framework. Mol Cancer Ther 10 (3), 416-426. https://doi.org/ 10.1158/1535-7163.MCT-10-0811.

Hyemin, P., Shangjin, K., Jinshang, K., Hyungsub, K., 2012. Reactive oxygen species mediated ginsenoside Rg3- and Rh2-induced apoptosis in hepatoma cells through

mitochondrial signaling pathways. Food Chem Toxicol 50 (8), 2736-2741. https://doi.org/10.1016/j.fct.2012.05.027.

Kang, J.H., Song, K.H., Woo, J.K., Park, M.H., Man, H.R., Choi, C., Oh, S.H., 2011. Ginsenoside Rp1 from Panax ginseng exhibits anti-cancer activity by down-regulation of the IGF-1R/Akt pathway in breast cancer cells. Plant Food Hum Nutr 66 (3), 298-305. https://doi.org/10.1007/s11130-011-0242-4.

Kashinath, M., Hemant, B., Praerna, C., Koka, P.S., 2013. Ayurveda for chemo-radiotherapy induced side effects in cancer patients. J Stem Cell 8 (2), 115-129. https://doi.org/jsc.2014.8.2.115.

Krieg, M., Fläschner, G., Alsteens, D., Gaub, B.M., Roos, W.H., Wuite, G.J.L., Gaub, H.E., Gerber, C., Dufrêne, Y.F., Müller, D.J., 2018. Atomic force microscopy-based mechanobiology. Nature Phys 1 (1), 41-57. https://doi.org/10.1038/s42254-018-0001-7.

Kim, E.J., Kwon, K.A., Lee, Y.E., Kim, J.H., Kim, S.H., Kim, J.H., 2018. Korean red ginseng extract reduces hypoxia-induced epithelial-mesenchymal transition by repressing NF-kappaB and ERK1/2 pathways in colon cancer. J Gins Res 42 (3), 288-297. https://doi.org/10.1016/j.jgr.2017.03.008.

Kim, K., Ahn, H.J., Lee, J.H., Kim, J.H., Yang, S.S., Lee, J.S., 2014. Cellular membrane collapse by atmospheric-pressure plasma jet. Appl Phys Lett 104 (1), 013701. https://doi.org/10.1063/1.4861373.

Kim, Y.S., Balaraju, K., Jeon, Y., 2017. Biological characteristics of bacillus amyloliquefaciens AK-0 and suppression of ginseng root-rot caused by

cylindrocarpon destructans. J Appl Microbiol. 122 (1), 166-179. https://doi.org/10.1111/jam.13325.

Kwon, K.R., Park, W.P., Kang, W.M., Jeon, E.Y., Jang, J.H., 2011. Identification and analysis of differentially expressed genes in mountain cultivated ginseng and moutain wild ginseng. J Acupunct Meridian Stud 4 (2), 123-128. https://doi.org/10.1016/S2005-2901(11)60018-6.

Lazar, P., Zhang, S., Safarova, K., Li. Q., Froning, J.P., Granatier, J., Hobza, P., Zboril, R., Besenbacher, F., Dong M.D., Otyepka, M., 2013. Quantification of the interaction forces between metals and graphene by quantum chemical calculations and dynamic force measurements under ambient conditions. ACS Nano 7 (2), 1646-1651. https://doi.org/10.1021/nn305608a.

Lee, H., Lee, S., Jeong, D., Kim, S.J., 2018. Ginsenoside Rh2 epigenetically regulates cell-mediated immune pathway to inhibit proliferation of MCF-7 breast cancer cells. J Gins Res 42 (4), 455-462. https://doi.org/10.1016/j.jgr.2017.05.003.

Li, Q., Liu, L., Zhang, S., Xu, M., Wang, X.Q., Wang, C., Besenbacher, F., Dong, M.D., 2014. Modulating $A\beta_{33\text{-}42}$ peptide assembly by graphene oxide. Chem-Eur J 20 (24), 7236-7240. https://doi.org/10.1002/chem.201402022.

Ma, Y.X., Feng, Q.Q., Ouyang, L.S., Mu, S.H., Liu, B.B., Li, Y.L., Chen, S., Lei, W.L., 2014. Morphological diversity of GABAergic and cholinergic interneurons in the striatal dorsolateral and ventromedial regions of rats. Cell Mol Neurobiol 34 (3), 351-359. https://doi.org/10.1007/s10571-013-0019-4.

Melak, M., Plessner, M., Grosse, R., 2017. Actin visualization at a glance. J Cell Sci

130 (3), 525-530. https://doi.org/10.1242/jcs.189068.

Nawab, J.D., Abid, H.,Muzamil, A., 2015. Pharmacologic overview of withania somnifera, the Indian ginseng. Cell Mol Life Sci 72 (23), 4445-4460. https://doi.org/10.1007/s00018-015-2012-1.

Pang, G., Wang, F., Zhang, L.W., 2018. Dose matters: Direct killing or immunoregulatory effects of natural polysaccharides in cancer treatment. Carbohydr Polym 195, 243-256. https://doi.org/10.1016/j.carbpol.2018.04.100.

Park, J.Y., Choi, P., Kim, H.K., Kang, K.S., Ham, J., 2016. Increase in apoptotic effect of Panax ginseng by microwave processing in human prostate cancer cells: invitro and invivo studies. J Gins Res 40 (1), 62-67. https://doi.org/10.1016/j.jgr.2015.04.007.

Peralta, E.A., Murphy, L.L., Minnis, J., Louis, S., Dunnington, G.L., 2009. American ginseng inhibits induced COX-2 and NFKB activation in breast cancer cells. J Surg Res 157 (2), 261-267. https://doi.org/10.1016/j.jss.2009.05.011.

Poudyal, D., Cui, X.L., Le, P.M., Hofseth, A.B., Windust, A., Nagarkatti, M., Nagarkatti, P.S., Schetter, A.J., Harris, C.C., Hofseth, L.J., 2013. A key role of microRNA-29b for the suppression of colon cancer cell migration by American ginseng. Plos One 8 (10), e75034. https://doi.org/10.1371/journal.pone.0075034.

Qi, L.W., Wang, C.Z., Yuan, C.Z., 2011. Ginsenosides from American ginseng: chemical and pharmacological diversity. Phytochemistry 72 (8), 689-699. https://doi.org/10.1016/j.phytochem.2011.02.012.

Rajeshwary, G, Gilda, JE, Gomes, AV., 2014. The necessity of and strategies for

improving confidence in the accuracy of western blots. Expert Rev Proteomic 11 (5): 549-560. https://doi.org/10.1586/14789450.2014.939635.

Shi, X., Yang, J., Wei, G., 2018. Ginsenoside 20(S)-Rh2 exerts anti-cancer activity through the Akt/GSK3β signaling pathway in human cervical cancer cells. Mol Med Rep 17 (3), 4811-4816. https://doi.org/10.3892/mmr.2018.8454.

Tai, C.J., Hsu, C.H., Shen, S.C., Lee, W.R., Jiang, M.C., 2010. Cellular apoptosis susceptibility (CSE1L/CAS) protein in cancer metastasis and chemotherapeutic drug-induced apoptosis. J Expe Clin Canc Res 29 (1), 110. https://doi.org/10.1186/1756-9966-29-110.

Torre, L.A., Bray, F., Siegel, R.L., Ferlay, J., Lortet-Tieulent, J., Jemal, A., 2015. Global cancer statistics, 2012. CA-Cancer J 65 (2), 87-108. https://doi.org/10.3322/caac.21262.

Virjula, S., Zhao, F.H., Leivo, J., Vanhatupa, S., Kreutzer, J., Vaughan, T.J., Honkala, A.M., Viehrig, M., Mullen, C.A., Kallio, P., 2017. The effect of equiaxial stretching on the osteogenic differentiation and mechanical properties of human adipose stem cells. J Mech Behav Biomed 72, 38-48. https://doi.org/10.1016/j.jmbbm.2017.04.016.

Wang, C.Z., Li, X.L., Wang, Q.F., Mehendale, S.R., Fishbein, A.B., Han, A.H., Sun, S., Yuan, C.S., 2009. The mitochondrial pathway is involved in American ginseng-induced apoptosis of SW-480 colon cancer cells. Oncol Rep 21 (3), 577-584. https://doi.org/10.3892/or_00000259.

Wang, Q.S., He, J.T., Meng, L.Y., Liu, Y.S., Pu, H., Ji, J.G., 2010. A proteomics analysis

of rat liver membrane skeletons: the investigation of actin- and cytokeratin-based protein components. J Proteome Res 9 (1), 22-29. https://doi.org/10.1021/pr900102n.

Wang, Y.Y., Huang, M.Y., Sun, R.L., Pan, L., 2015. Extraction, characterization of a ginseng fruits polysaccharide and its immune modulating activities in rats with Lewis lung carcinoma. Carbohydr Polym 127, 215-221. https://doi.org/10.1016/j.carbpol.2015.03.070.

Wong, A.S., Che, C.M., Leung, K.W., 2015. Recent advances in ginseng as cancer therapeutics: a functional and mechanistic overview. Nat Prod Rep 32 (2), 256-72. https://doi.org/10.1039/c4np00080c.

Yang, C.X., Gou, Y.Q., Chen, J.Y., An, J., Chen, W.X., Hu, F.D., 2013. Structural characterization and antitumor activity of a pectic polysaccharide from codonopsis pilosula. Carbohydr Polym 98 (1), 886-895. https://doi.org/10.1016/j.carbpol.2013.06.079.

Yang, L., Liu, X.Z., Lu, Z.B., Chan, J.Y.W., Zhou, L.L., Fung, K.P., Wu, P., Wu, S.H., 2010. Ursolic acid induces doxorubicin-resistant HepG2 cell death via the release of apoptosis-inducing factor. Cancer Lett 298 (1), 128-138. https://doi.org/10.1016/j.canlet.2010.06.010.

Yoon, J.H., Choi, Y.J., Lee, S.G., 2012. Ginsenoside Rh1 suppresses matrix metalloproteinase-1 expression through inhibition of activator protein-1 and mitogen-activated protein kinase signaling pathway in human hepatocellular carcinoma cells. Eur J Pharmacol 679 (1-3), 24-33.

https://doi.org/10.1016/j.ejphar.2012.01.020.

Yu, T., Yang, Y.Y., Kwak, Y.S., Song, G.G., Kim, M.Y., Rhee, M.H., Cho, J.Y., 2017. Ginsenoside Rc from Panax ginseng exerts anti-inflammatory activity by targeting TANK-binding kinase 1/interferon regulatory factor-3 and p38/ATF-2. J Gins Res 41 (2), 127-133. https://doi.org/10.1016/j.jgr.2016.02.001.

Zhang, Z., Song, J., Besenbacher, F., Dong, M.D., Gothelf, K.V., 2013. Self-assembly of DNA origami and single-stranded tile structures at room temperature. Angew Chem Int Edit 52 (35), 9219-9223. https://doi.org/10.1002/anie.201303611.